

Luminescence of Fe-Doped Willemite Single Crystals

Enrico Cavalli,¹ Alessandro Belletti, and Ester Zannoni

Dipartimento di Chimica Generale ed Inorganica, Chimica Analitica e Chimica-Fisica, Università di Parma, Viale delle Scienze, 43100 Parma, Italy

Received June 23, 1994; in revised form October 18, 1994; accepted October 24, 1994

The emission and excitation spectra of Fe-doped Zn_2SiO_4 (willemite) crystals were measured at temperatures ranging from 10 to 298 K. The luminescence consists of two contributions, both of broadband type: an emission due to the ${}^4T_1({}^4G) \rightarrow {}^6A_1({}^6S)$ interconfigurational transition of the d^5 Fe^{3+} ions in sites having approximate tetrahedral coordination and a second emission probably due to lattice defects induced by the requirement of charge compensation. The excitation spectrum of Fe^{3+} has been assigned on the basis of the ligand field theory, and the energies of the bands have been fitted with the following values of the ligand field parameters: $Dq = 743 \text{ cm}^{-1}$, $B = 535 \text{ cm}^{-1}$, and $C = 3155 \text{ cm}^{-1}$. From these data, it is reasonable to suppose that the Fe^{3+} ions responsible for the emission are located at the Si^{4+} distorted tetrahedral sites. © 1995 Academic Press, Inc.

INTRODUCTION

The emission properties of the transition metal ions are of great interest, as they can find application in the development of tunable solid-state lasers, phosphors, etc. Among the emitting ions, Fe^{3+} is one of the less studied; its emission, in fact, is known, but not very common, and arises mainly from ions in tetrahedral sites (1–5, 8–10), even if luminescence from octahedral sites has also been observed (6, 7). Several studies were carried out in the 1970s on powdered samples of LiM_3O_8 ($M = \text{Al}, \text{Ga}$), $M'\text{AlO}_2$ ($M' = \text{Li}, \text{Na}, \text{K}$) (1–4), and YAG(5), in which Fe^{3+} was demonstrated to be a good activator. Up to now, however, only a few iron-doped laser crystals have been characterized; spinel, ackermanite (9), and forsterite (10) are those most recently studied. In particular, in their paper on $\text{Mg}_2\text{SiO}_4:\text{Fe}$, Walker *et al.* (10) suggested that the emission in the 800–900 nm region arises from Fe^{3+} occupying the tetrahedral Si sites, even if the ferric ions tend to occupy preferentially the octahedral Mg sites (11). Therefore, it has seemed interesting to us to verify the optical behavior of Fe^{3+} in silicates having only tetrahedral sites. In this work, we report for the first time, to

our knowledge, the emission properties of iron-doped willemite (Zn_2SiO_4) single crystals. When compared with results from previous papers (1–10) on the emission of Fe^{3+} , our spectra show several unexpected features. A general picture, giving a reasonable explanation for most of them, is proposed.

EXPERIMENTAL

(1) Synthesis and Crystal Data

Pale yellowish $\text{Zn}_2\text{SiO}_4:\text{Fe}$ single crystals ($5 \times 2 \times 1$ mm) of good optical quality have been grown by the flux method (12) using Li_2MoO_4 as solvent in the temperature range 1400–800°C. A nominal $\text{Fe}:\text{Zn} = 1:100$ molar ratio was used. The structure was confirmed by X-ray powder diffraction.

Willemite, Zn_2SiO_4 , is hexagonal, space group $R\bar{3}$, with cell parameters $a = 13.948 \text{ \AA}$ and $c = 9.315 \text{ \AA}$ (13). In the layered structure of the willemite (14), the oxygen atoms located along the c -axis are surrounded by a Zn(1)–Zn(2)–Si triangle perpendicular to the axis, each cation being in a tetrahedral environment of oxygen atoms. These tetrahedra are also superimposed in such a way that along the c -axis we can find a Zn(1)–Zn(2)–Si sequence. The two tetrahedral zinc sites, $\text{Zn}(1)\text{O}_4$ and $\text{Zn}(2)\text{O}_4$, are both distorted (C_1 real point symmetry), the former with a Zn–O average distance of 1.9495 Å and slightly more distorted with respect to the latter, whose Zn–O average distance is equal to 1.9611 Å. The average Si–O distance in the SiO_4 distorted tetrahedron is 1.6346 Å. On the basis of the ionic radii IR-reported by Shannon and Prewitt (15), we can say that the Fe^{3+} ions (IR = 0.49 Å) should prefer the Zn^{2+} (IR = 0.60 Å) sites, even if the Si^{4+} (IR = 0.26 Å) sites are partially occupied (11).

(2) Optical Measurements

Emission and excitation spectra were measured using, as a source, a 450 W xenon lamp fitted with a Spex Minimate 0.25-m monochromator and suitable filters to isolate the wavelengths of interest; the emission was analyzed with a Spex 1.26-m monochromator and detected by a

¹ To whom correspondence should be addressed.

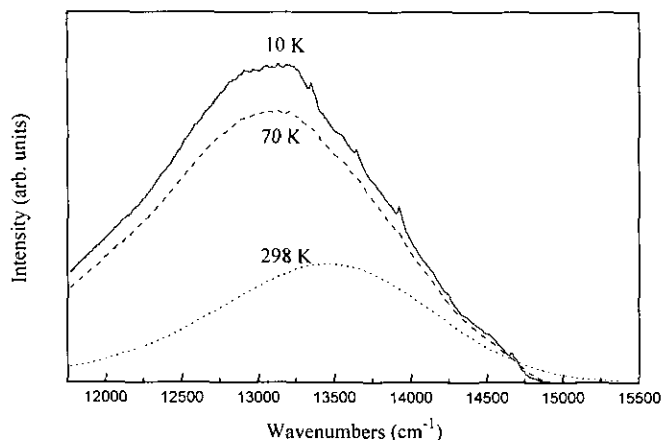


FIG. 1. Emission spectrum of Fe^{3+} -doped willemite at different temperatures, with excitation at $22,200 \text{ cm}^{-1}$ (450 nm).

cooled RCA C31034 photomultiplier. The spectra were not corrected for the system responsiveness. For the decay curves measurements, the excitation at 355 nm was provided by a pulsed Nd-YAG laser (Quanta System Model GYL 102); the emission was isolated by means of a Hilger-Watts Model D330 double monochromator and detected with a cooled Hamamatsu Model R943-02 photomultiplier connected to a LeCroy 9410 transient digitizer. The samples were cooled by means of an Air Products Displex DE 202 or a Galileo Vacuum Tech Model K1 closed-cycle cryostat.

RESULTS AND DISCUSSION

The luminescence spectra of $\text{Zn}_2\text{SiO}_4:\text{Fe}$ at 10, 70, and 298 K, with excitation at $22,200 \text{ cm}^{-1}$ (450 nm), are shown in Fig. 1. The following points are to be outlined:

—The emission at low temperature is of broadband type, with a maximum at about $13,100 \text{ cm}^{-1}$, and a vibrational progression on its high-energy side, with frequency of $\sim 250 \text{ cm}^{-1}$.

—the intensity of the emission decreases as the temperature increases, at 10 K being about three times more intense than at 298 K. Moreover, the emission maximum shifts from $\sim 13,100 \text{ cm}^{-1}$ at 10 K to $\sim 13,500 \text{ cm}^{-1}$ at 298 K.

—the decay curves measured at different wavelengths are nonexponential and hard to deconvolute. In any case, the 10-K emission at higher energy ($13,300\text{--}13,800 \text{ cm}^{-1}$) is much slower than that at lower energy ($11,700\text{--}12,500 \text{ cm}^{-1}$): two approximate lifetimes have been calculated for the former, about 5 and 2 msec, and only one for the latter, about $50 \mu\text{sec}$.

We point out that previous papers on the luminescence of Fe^{3+} (1-4, 8, 10) report quite different behaviors: the

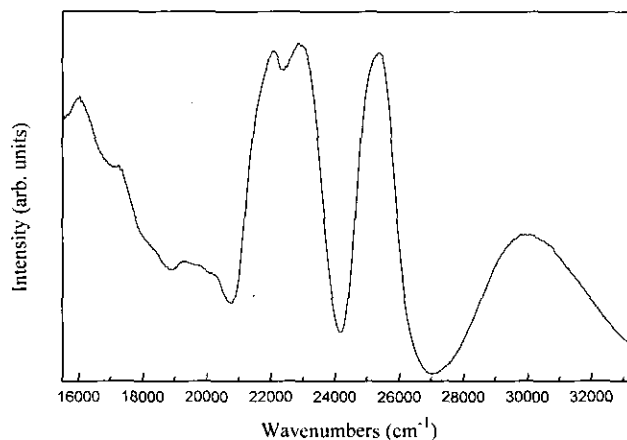


FIG. 2. 10-K excitation spectrum, with emission at $13,700 \text{ cm}^{-1}$.

low-temperature spectra are usually made up of sharp zero-phonon lines (the so-called *R* lines) plus sidebands, and the emission intensities are almost independent of the temperature.

The excitation spectra have been recorded at 10 K for several emission wavelengths; as can be seen in Fig. 2 (emission at $13,700 \text{ cm}^{-1}$) and in Fig. 3 (emission at $11,700 \text{ cm}^{-1}$), we are in the presence of two different kinds of spectra. By selecting the excitation wavelengths with care, it is possible to separate the two emissions; these are shown in Figs. 4a and 4b. In the following, we will discuss them separately, and for this purpose, we will indicate as luminescence 1 the emission shown in Fig. 4a and its related excitation, see Fig. 2, and as luminescence 2 the emission in Fig. 4b and the excitation in Fig. 3.

Luminescence 1

This emission spectrum consists of a broadband with a maximum at $13,450 \text{ cm}^{-1}$, which can be assigned to the

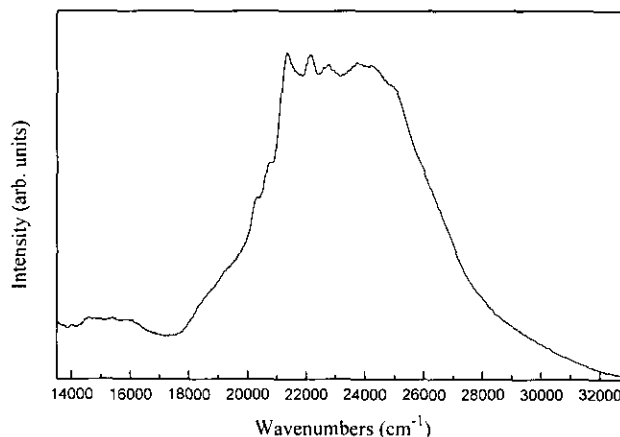


FIG. 3. 10-K excitation spectrum, with emission at $11,700 \text{ cm}^{-1}$.

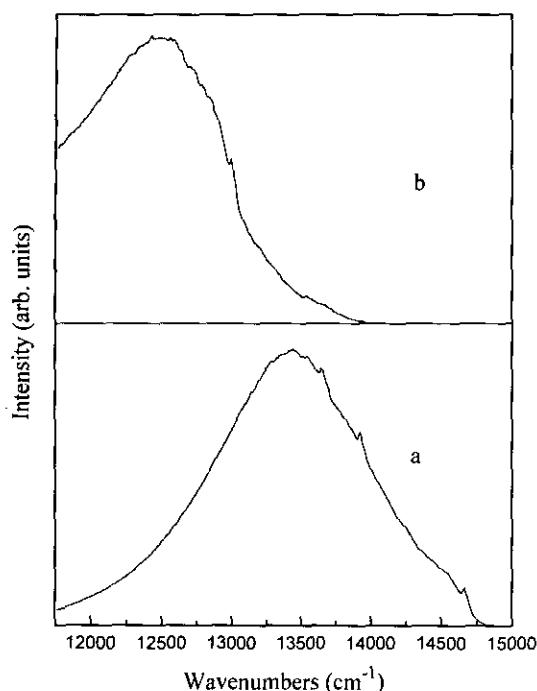


FIG. 4. 10-K emission spectrum, with excitation at (a) 32,000 cm^{-1} and (b) 24,200 cm^{-1} .

${}^4T_1({}^4G) \rightarrow {}^6A_1({}^6S)$ transition of the $d^5 \text{Fe}^{3+}$ ions, having distorted tetrahedral coordination. In T_d symmetry, this transition is both symmetry and spin-forbidden, and occurs as a consequence of the spin-orbit coupling (8). The vibrational progression on the high-energy side of the band is due to a localized mode with energy of about 250 cm^{-1} . In the excitation spectrum (see below), the maximum of the ${}^4T_1({}^4G) \leftarrow {}^6A_1({}^6S)$ lies at about 16,000 cm^{-1} , then the Stokes shift is 2550 cm^{-1} . From these data, we can easily obtain the Huang-Rhys factor, whose value of about 5 is in good agreement with the shape of the emission band. Concerning the temperature dependence, the intensity of the 10 K emission reduces to about 30% at 298 K, and the shift of its maximum is negligible. This indicates that, as the temperature raises, nonradiative processes become active.

The main features of the excitation spectrum (Fig. 2) are reported in Table 1, together with our assignments. These have been made mainly by considering the papers of Pott *et al.* (3, 4), McShera *et al.* (8), and Walker *et al.* (10), and deserve some comments.

In fact, these papers report emission spectra of tetrahedral Fe^{3+} of R lines plus sidebands type, with a quite small Stokes shift, on the order of 800–1000 cm^{-1} . On the contrary, we are in the presence of a broadband emission, with no visible zero-phonon lines; as a consequence, we have to expect a larger value of the Stokes shift. The assignment of the maximum at 15,974 cm^{-1} to the

${}^4T_1({}^4G) \leftarrow {}^6A_1({}^6S)$ leads to a Stokes shift of about 2500 cm^{-1} , in good agreement with the emission bandshape.

The ${}^4T_2({}^4G) \leftarrow {}^6A_1({}^6S)$ transition usually occurs as a broadband lying at about 3000–4000 cm^{-1} from the ${}^4T_1({}^4G) \leftarrow {}^6A_1({}^6S)$ and with similar intensity (3, 4, 8). In our spectrum, we can observe two shoulders on the high-energy side of the first excitation band, at 17,270 and 18,330 cm^{-1} , respectively, and a weak band with two maxima at 19,305 and 20,263 cm^{-1} . These maxima tend to become sharp peaks in the excitation spectra at different emission wavelengths. It seems to us reasonable to assign the first shoulder to a component of the ${}^4T_1({}^4G) \leftarrow {}^6A_1({}^6S)$ and the second one to the ${}^4T_2({}^4G) \leftarrow {}^6A_1({}^6S)$ transition, even if a nonnegligible superposition of the two bands should occur. The features at 19,305 and 20,263 cm^{-1} could be assigned, on the basis of their positions, to doublet transitions; but on the other hand, such transitions have never been observed in previous spectra and their assignment remains uncertain.

The ${}^4A_1, {}^4E({}^4G) \leftarrow {}^6A_1({}^6S)$ transition is usually indicated as a weak band (10), or a shoulder (3, 4, 8) on the low-energy side of the more intense band, which is often split in two or more components, assigned to the ${}^4T_2({}^4D) \leftarrow {}^6A_1({}^6S)$ transition. On this basis, the shoulder at about 21,500 cm^{-1} can be assigned to the former transition and the remainder of the band, having maxima at 22,026 and 22,852 cm^{-1} , to two components of the latter.

Finally, the relatively sharp band centered at 25,348 cm^{-1} and the broadband with maximum at 29,940 cm^{-1} are to be assigned to the ${}^4E({}^4D) \leftarrow {}^6A_1({}^6S)$ and to the ${}^4T_1({}^4P) \leftarrow {}^6A_1({}^6S)$ transitions, respectively. The mean energies of the bands can be reasonably reproduced by diagonalization of the ligand field matrices for a d^5 ion, using the following values for the parameters:

$$Dq = 743 \text{ cm}^{-1}; \quad B = 535 \text{ cm}^{-1}; \quad C = 3155 \text{ cm}^{-1}.$$

This fit has to be considered only as indicative; in fact,

TABLE 1
Spectral Features and Assignments in the 10-K Fe^{3+} Excitation Spectrum ($\bar{\nu}_{\text{obs.}} = 13,700 \text{ cm}^{-1}$)

$\bar{\nu}$ (cm^{-1})	Intensity	Assignment
15,974	Broadband max.	${}^4T_1({}^4G) \leftarrow {}^6A_1({}^6S)$
17,270	Shoulder	Component
18,330	Shoulder	${}^4T_2({}^4G) \leftarrow {}^6A_1({}^6S)$
19,305	Weak band	Doublet components
20,263	Weak band	(?)
21,500	Shoulder	${}^4A_1, {}^4E({}^4G) \leftarrow {}^6A_1({}^6S)$
22,026	Strong max.	${}^4T_2({}^4D) \leftarrow {}^6A_1({}^6S)$
22,852	Strong max.	Component
25,348	Strong max.	${}^4E({}^4D) \leftarrow {}^6A_1({}^6S)$
29,940	Broadband max.	${}^4T_1({}^4P) \leftarrow {}^6A_1({}^6S)$

there are effects which have not been taken into account in the calculations, but which play a significant role in determining the energies of the states, such as the covalency effects and the Racah–Trees correction, as pointed out by Curie *et al.* (16) for the Mn^{2+} ions, and, to a lesser extent, the spin–orbit coupling. Nevertheless, this result confirms the correctness of our assignments and allows us to draw some considerations:

—the emission is at higher energy than in Mg_2SiO_4 , in agreement with the lower strength of the ligand field (10). If we take into account the ionic radii and a statistical distribution of the dopant, it is reasonable to suppose that the Fe^{3+} ions lie preferably at the Zn sites, even if the Si sites are partially occupied (11). Previous papers on the luminescence of Fe^{3+} (3–6, 8, 10), report Dq values ranging from 700 to 800 cm^{-1} for ions lying in smaller cavities than those of Zn in willemite; due the strong dependence of the ligand field strength on the metal–ligand distance, we should expect a quite smaller Dq value for Fe^{3+} at the zinc sites. Thus, we can suppose that the emission arises mainly from iron ions at the Si sites. Moreover, we have to consider that the substitution of the Zn^{2+} or Si^{4+} ions for Fe^{3+} requires charge compensation, which can be achieved both by the inclusion of Li^+ ions (from the flux) and by the formation of vacancies; it is then evident that the Fe^{3+} ions can experience several different local fields. This fact causes the broadening and the superposition of the bands and the occurrence of several lifetimes, and complicates the understanding of the experimental results.

—the strong diminution of the B parameter with respect to the free-ion value, is indicative of a nonnegligible covalent character of the metal–ligand bonds, as stated above;

—the broadband shape of the emission indicates a strong difference in the electron–phonon coupling between the ground and the excited state.

Luminescence 2

This is an unexpected emission; to understand it, a number of experiments have been made, which did not lead to definitive conclusions, unfortunately. In the following, we briefly describe the most significant conclusions:

—pure flux-grown Zn_2SiO_4 shows only an emission in the visible region, which can be attributed to MoO_4^{2-} ions, certainly present as an impurity arising from the solvent;

—powdered samples of $Zn_2SiO_4:Fe$ prepared by solid-state reaction at 1200°C (starting from ZnO , SiO_2 , and Fe_2O_3 in appropriate amounts) did not show any emission;

—flux-grown Zn_2SiO_4 crystals doped with Cr, Mn, Ni, and Co (the most probable unwanted dopants) have completely different optical spectra than $Zn_2SiO_4:Fe$;

—attempts to grow more concentrated crystals of $Zn_2SiO_4:Fe$ were unsuccessful.

Therefore, this emission can be attributed neither to Fe^{3+} ions, the shape of the excitation spectrum being too different from those typical of iron, nor to Fe^{2+} ions, which strongly prefer octahedral sites and whose emission lies at lower energies (10). Moreover, the emission from Fe pairs cannot be taken into account, due to the concentration of the dopant being very low, as well as emissions from unwanted impurities, the most probable of which have different optical properties. Thus, it should be due to defects originating in the melt as an effect of the charge compensation required by the presence of Fe^{3+} in the host lattice.

Finally, we must point out that the luminescence 2 is completely quenched at room temperature; this is due, in part, to both quenching of the total emission and of the shift of the maximum shown in Fig. 1.

CONCLUSIONS

Two different emissions occur in the luminescence spectrum of Fe-doped willemite. The one at longer wavelengths and with a lifetime of about 50 μ sec arises probably from lattice defects originating in the melt; that at shorter wavelengths and with lifetimes of 2 and 5 msec is due to the Fe^{3+} ions in tetrahedral sites. The excitation spectrum of this emission is consistent with that of a d^5 ions, and the assignments are in good agreement with those reported in previous papers.

The broadband-type Fe emission is fundamentally different from the zero-phonon line plus sidebands type emission of the same ion in forsterite and, in general, in other host lattices. This implies that the mutual positions of the ground and the excited states (in a single conformational coordinate scheme), as well as the difference in electron–lattice coupling between the two states, are very different in the two cases. This situation could be connected to the greater covalent character of the Fe–O bonds in willemite than those in forsterite, as evidenced by the lower value of the B interelectronic interaction parameter, and by the higher value of the Huang–Rhys parameter.

ACKNOWLEDGMENTS

We thank Professor L. Oleari and Professor M. Bettinelli for encouragement and helpful discussions. This work was done with the financial support of CNR (Italian National Research Council) within the "Progetto Finalizzato Materiali Speciali" (Contracts 93.01218.PF68 and 92.00907.PF68)

REFERENCES

1. N. T. Melamed, P. J. Viccaro, J. O. Artman, and F. S. de S. Barros, *J. Lumin.* **1** and **2**, 348 (1970).

2. D. T. Palumbo, *J. Lumin.* **4**, 89 (1971).
3. G. T. Pott and B. D. McNicol, *Chem. Phys. Lett.* **12**, 62 (1971).
4. G. T. Pott and B. D. McNicol, *J. Chem. Phys.* **56**, 5246 (1972).
5. Yu. A. Voitukevitch, M. V. Korzhik, V. V. Kuzmin, M. G. Livshits, and M. L. Meilman, *Opt. Spektrosk.* **63**, 480 (1987).
6. N. T. Melamed, J. M. Neto, T. Abritta, and F. S. de S. Barros, *J. Lumin.* **24, 25**, 249 (1981).
7. G. O'Connor, C. McDonagh, and T. J. Glynn, *J. Lumin.* **48, 49**, 545 (1991).
8. C. McShera, P. J. Colleran, T. J. Glynn, G. F. Imbusch, and P. Remeika, *J. Lumin.* **28**, 41 (1983).
9. R. Clausen and K. Petermann, *J. Lumin.* **40, 41**, 185 (1988).
10. G. Walker and T. J. Glynn, *J. Lumin.* **54**, 131 (1991).
11. J. M. Gaite and S. S. Hafner, *J. Chem. Phys.* **80**, 2747 (1984).
12. K. Watanabe, *J. Cryst. Growth* **114**, 373 (1991).
13. K. H. Klaska, J. C. Eck, and D. Pohl, *Acta Crystallogr. Sect. B* **34**, 3324 (1978).
14. Chin' Hang, M. A. Simonov, and N. V. Belov, *Sov. Phys. Crystallogr. Engl. Transl.* **15**, 387 (1970).
15. R. D. Shannon and C. T. Prewitt, *Acta Crystallogr. Sect. B* **25**, 925 (1969).
16. D. Curie, C. Bartou, and B. Canny, *J. Chem. Phys.* **61**, 3048 (1974).